Characterisation of the active phase in caesium-doped iron–vanadium-oxide catalysts for the selective oxidation of polyaromatics

Andrew P.E. York[a,*], Angelika Brückner[a], Peter-Michael Wilde[b], Hartmut Mehner[c], Martin Kraum[d] and Manfred Baerns[d,‡]

[a] *Institut für angewandte Chemie Berlin-Adlershof e.V., Rudower Chaussee 5, D-12484 Berlin, Germany*
[b] *Gesellschaft zur Förderung angewandte Optik, Optoelektronik und Spektroskopie (GOS), Rudower Chaussee 5, D-12484 Berlin, Germany*
[c] *Bundesanstalt für Materialforschung und -prüfung, Rudower Chaussee 5, D-12484 Berlin, Germany*
[d] *Ruhr-Universität Bochum, Lehrstuhl für Technische Chemie, D-44780 Bochum, Germany*

Received 22 July 1996; accepted 29 October 1996

The addition of caesium sulphate to unsupported vanadium–iron-oxide materials leads to the formation of an amorphous non-stoichiometric phase, as well as the crystalline phases, $FeVO_4$, $Fe_2V_4O_{13}$, and $Fe_{1-X}S$ (pyrrhotite). Caesium was only present in the amorphous parts of the sample, and the amount of the new phase formed was found to vary depending on the vanadium: iron ratio and the amount of caesium dopant added. The new phase contains Fe^{3+} ions with oxide lattice vacancies in their coordination sphere, i.e. Fe^{3+}–$V_O(e^-)$ species. Catalytic testing demonstrated that the caesium-doped samples were more selective for the oxidation of fluorene to 9-fluorenone. The role of the caesium is probably to modify the surface acidity of the catalyst and act in the formation of stable oxide lattice vacancies.

Keywords: selective oxidation, polyaromatics, Cs-doped iron vanadates, iron sulphide

1. Introduction

The selective oxidation of polyaromatics (e.g. anthracene, fluorene) to ketones and anhydrides is of considerable industrial and academic interest, and various vanadium-oxide-based catalysts have been used for these reactions [1]. For example, Majunke et al. studied the oxidation of fluorene over unsupported vanadium–iron-oxide catalysts and found that the addition of caesium leads to an increase in the selectivity to 9-fluorenone from 60 to > 95% [2–5]. This improvement was explained by changes in the acid–base properties of the catalyst surface on the addition of alkali metal, assuming that a decrease in Lewis-acid sites weakens the adsorptive bonding of the basic hydrocarbon to the surface and, therefore, decreases the amount of total oxidation. However, Brückner and co-workers have studied the same catalysts using electron spin resonance spectroscopy (ESR) and found that those catalysts doped with caesium exhibit a low-field ESR signal ($g' \approx 18$), which does not appear in the undoped samples [6–8]. Subjecting the samples to temperature changes or applying external mechanical pressure, while measuring the ESR spectra, the new low-field signal was attributed to an Fe^{3+} cation located in close proximity to an oxygen vacancy occupied by an electron, i.e. Fe^{3+}–$V_O(e^-)$ species; these species have also been observed in other oxidic systems, such as iron-doped $BaTiO_3$ [9]. It was proposed that this new phase was important in the improved selectivities observed.

Despite this earlier work, the morphology of the caesium-doped vanadium–iron-oxide catalysts is still unknown and the nature of the catalytically active sites unclear. Furthermore, these catalysts were prepared using non-standardised procedures [7], by which the composition might have been altered; we have studied a more complete series of vanadium–iron-oxide catalysts, prepared by a standard method. Scanning electron microscopy (SEM) and energy dispersive X-ray analyses (EDX) have been carried out, and catalytic tests have been performed to confirm the conclusions from the characterisation study.

2. Experimental

2.1. Catalyst preparation

Materials with V : Fe atomic ratios of 1 : 0.13 to 1 : 2.0 were prepared from mixed aqueous solutions of ammonium metavanadate (NH_4VO_3) and iron chloride ($FeCl_3 \cdot 6H_2O$) by co-precipitation with concentrated NH_3. Cs-, Rb- and K-doped catalysts were prepared by the addition of the alkali metal sulphate (M_2SO_4) to the

* To whom correspondence should be addressed. Current address: Inorganic Chemistry Laboratory, University of Oxford, South Parks Road, Oxford OX1 3QR, UK.
‡ Current address: Institut für angewandte Chemie Berlin-Adlershof e.V., Rudower Chaussee 5, D-12484 Berlin, Germany.

mixed solution before the precipitation step. The precipitated samples were filtered, dried by rotary evaporation and calcined for 18 h at 623 K. Pure $FeVO_4$ was synthesised according to the method described by Touboul and co-workers [10,11] and Mössbauer spectroscopy showed that only 4% α-Fe_2O_3 was present as impurity.

2.2. Catalyst characterisation

The crystalline components of the materials were identified by X-ray diffraction (XRD) with Cu-Kα radiation. ESR and transmission Mössbauer spectra were recorded as published previously [6], and details of the conversion electron Mössbauer spectroscopy were given earlier by Meisel and co-workers [12,13]. SEM was carried out using a Zeiss DSM 962 microscope and EDX using a Noran Voyager instrument and Proza software for ZAF correction. The BET surface areas of all the catalysts were essentially constant, only ranging from < 1 to 2.2 $m^2\ g^{-1}$.

2.3. Catalytic testing

Fluorene was oxidised with air in a fixed-bed quartz reactor ($d = 8$ mm, $l = 300$ mm) which was described in detail previously [14]. The product distribution obtained in the oxidation experiments was determined by GC (Siemans Sichromat 2) and HPLC (WATERS 712, UV array detector) analysis. For details of the product analysis see ref. [15].

3. Results

3.1. X-ray diffraction, ESR spectroscopy and Mössbauer spectroscopy

A series of materials were prepared with varying vanadium : iron ratios. The amount of caesium dopant was kept constant, unless stated otherwise.

3.1.1. Effect of varying the iron content

The XRD data obtained for the various caesium-doped materials (table 1) shows that, as the iron content is increased, the most important phase observed changes from $Fe_2V_4O_{13}$ to $FeVO_4$, and finally α-Fe_2O_3 when the iron is in excess. Comparison of the caesium-doped and undoped V : Fe = 1 : 1 materials showed that no new crystalline phases are formed by the addition of caesium.

The ESR spectra of the caesium-doped materials show two signals at effective g values of $g' \approx 2$ and $g' \approx 18$, corresponding to the crystalline iron vanadates [6–8], and a new amorphous phase which does not appear in the undoped samples, respectively. The signal at $g' \approx 18$ does not appear in the spectra of either caesium- doped Fe_2O_3 or V_2O_5, prepared by the same precipitation method as the mixed oxide materials, demonstrating that the new phase contains both vanadium and iron, and can be regarded as $Fe_xV_yO_z$. The relative intensity of this low-field line and, thus, the percentage of the new phase, rises with increasing iron and constant caesium content, reaching a maximum for the V : Fe : Cs = 1 : 0.74 : 0.06 sample and slowly decreasing again (see table 1); it is important to note that Baerns and co-workers found that the most selective catalysts, for the selective middle-ring oxidation of polyaromatics, were the caesium-doped samples with V : Fe ratios between 1 : 0.75 and 1 : 1.4 [2–5], i.e. those with a high amount of the new phase and $FeVO_4$ as the main crystalline phase.

The Mössbauer spectra obtained for a number of the caesium-doped samples are shown in fig. 1, together with those for pure amorphous and crystalline $FeVO_4$. The spectrum of the vanadium-rich sample displays a single doublet, due to $Fe_2V_4O_{13}$ [7]. However, in the spectra for the samples with higher iron content, this single doublet

Table 1
XRD and ESR data for the various V : Fe : M materials (ESR data was taken at room temperature and is mass normalized)

Sample V : Fe : M [a]	Crystalline phases		
	major	minor	$I_{g' \approx 18}$ [b]
1 : 1.0 : 0	$FeVO_4$	α-Fe_2O_3 [c]	0.0
1 : 0.13 : 0.06 (Cs)	$Fe_2V_4O_{13}$, V_2O_5	unknown	3.3
1 : 0.30 : 0.06 (Cs)	$Fe_2V_4O_{13}$	unknown	11.7
1 : 0.60 : 0.06 (Cs)	$Fe_2V_4O_{13}$	$FeVO_4$	284.4
1 : 0.74 : 0.06 (Cs)	$FeVO_4$, $Fe_2V_4O_{13}$	–	1001.0
1 : 1.0 : 0.06 (Cs)	$FeVO_4$	α-Fe_2O_3 [c]	827.6
1 : 1.4 : 0.06 (Cs)	$FeVO_4$	α-Fe_2O_3	627.4
1 : 2.0 : 0.06 (Cs)	$FeVO_4$, α-Fe_2O_3	–	455.2
1 : 0.74 : 0.06 (Rb)	$FeVO_4$, $Fe_2V_4O_{13}$	–	13.5
1 : 0.74 : 0.06 (K)	$FeVO_4$, $Fe_2V_4O_{13}$	–	0.0

[a] Alkali metal dopant listed in parentheses.
[b] Relative intensity of the $g' \approx 18$ ESR peak.
[c] Small amount.

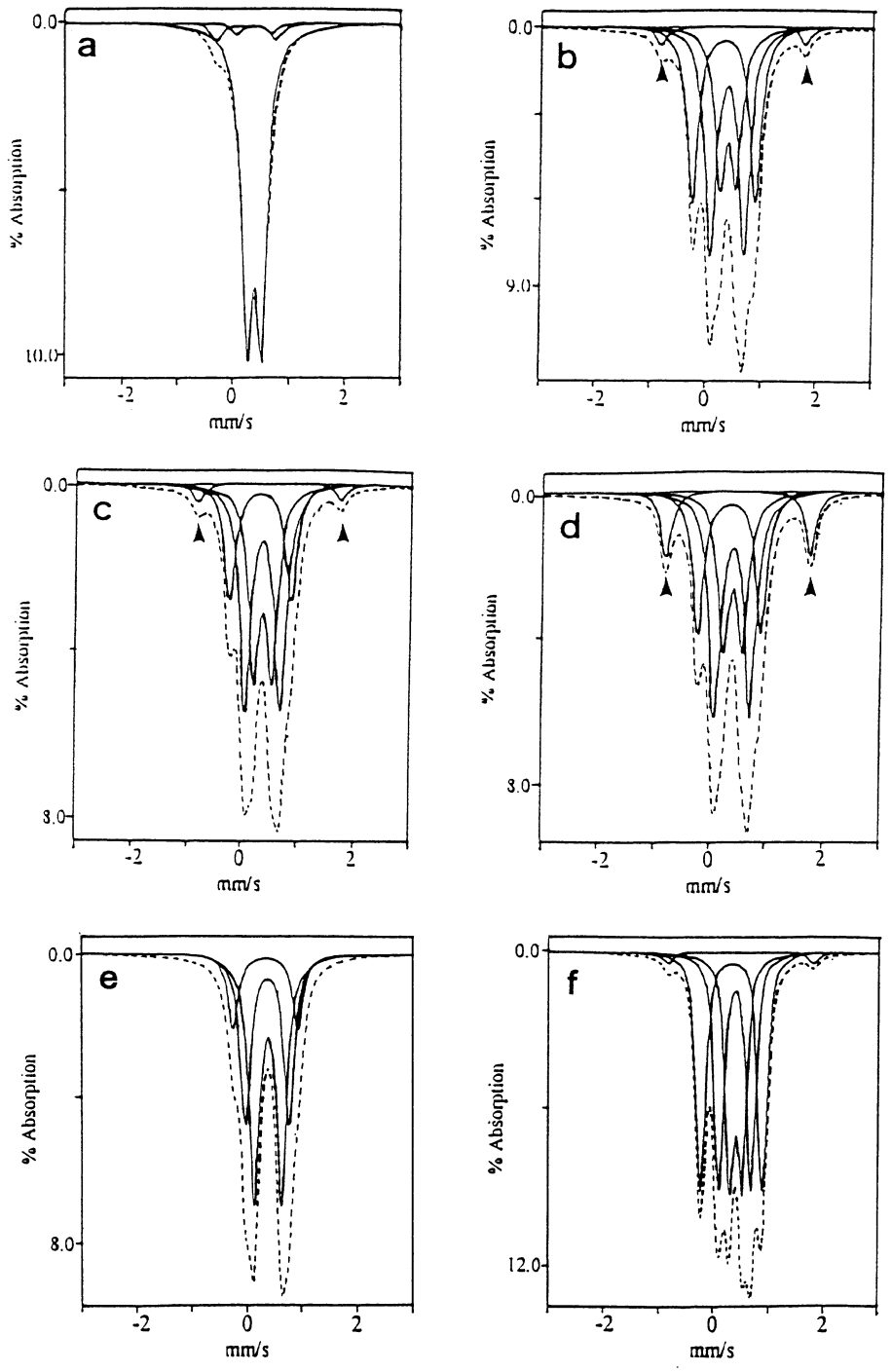

Fig. 1. Mössbauer spectra for various caesium-doped samples (Cs content is 0.06 mol% for all) and undoped iron vanadates: (a) V : Fe = 1 : 0.3; (b) V : Fe = 1 : 1; (c) V : Fe = 1 : 1.4; (d) V : Fe = 1 : 2; (e) $FeVO_4$ amorphous; and (f) $FeVO_4$ crystalline.

disappears and the presence of further doublets can be seen. The outer peaks (marked by the arrows) are the inner signals of the hyperfine sextet due to α-Fe_2O_3 (other four peaks out of range). The other three doublets can be assigned to a mixture of $FeVO_4$ and the amorphous $Fe_xV_yO_z$ phase, since the spectra obtained for pure amorphous (precursor) and crystalline $FeVO_4$ (figs. 1e and 1f) are also composed of three doublets [16]. Further, the isomer shifts and quadrupole splittings in the spectra of pure $FeVO_4$ were approximately the same as those for the caesium-doped samples. However, in the former the two doublets with larger quadrupole splittings, representing Fe^{3+} ions in more distorted surroundings, have higher intensities, indicating that the amorphous $Fe_xV_yO_z$ phase probably bears some similarity to the structure of $FeVO_4$ but has more distorted iron sites. This agrees with the assignment of the characteristic ESR signal at $g' \approx 18$ to Fe^{3+} centres, the coordina-

tion sphere of which is distorted by the presence of oxide vacancies.

3.1.2. Formation, characterisation and role of $Fe_{1-X}S$

When surface sensitive conversion electron Mössbauer spectroscopy is used to record the spectra, an additional hyperfine sextet, corresponding to $Fe_{1-X}S$ (pyrrhotite) [17,18] is observed in certain cases (fig. 2). In agreement with previous investigations [13], it appears only in samples with high caesium content. Since the caesium dopant is introduced as caesium sulphate, it is likely that the $Fe_{1-X}S$ is formed in the calcination process, by reduction of the sulphate with ammonia eliminated during the decomposition of the precursor.

To confirm that the formation of the new phase did not depend on the presence of sulphur, an iron–vanadium-oxide material was prepared using CsCl as the dopant. Also, a material was prepared using $(NH_4)_2SO_4$ as dopant, in order to introduce sulphur alone, without an alkali metal. The ESR spectrum of the sample doped with CsCl showed the characteristic signal of the new phase at $g' \approx 18$, the magnitude of which was similar to that in the material doped with Cs_2SO_4. In contrast, the sample with no caesium, prepared from $(NH_4)_2SO_4$, gave no low-field signal at $g' \approx 18$. Therefore, it can be concluded that the sulphur has no contribution to the low-field ESR signal, and is only a by-product of the reactions between the iron, vanadium and caesium compounds during calcination.

3.1.3. Effect of varying the caesium content

A series of materials with V : Fe = 1 : 0.74 and varying caesium content were synthesised, and the ESR spectra recorded. From fig. 3, it can be seen that, as the caesium is added up to 0.2 mol% (based on vanadium), a rapid increase in the relative intensity of the $g' \approx 18$ peak occurs, and a more gradual increase is observed from 0.2 to 0.5 mol%. It is proposed that the low-field ESR signal is caused by a phase formed when caesium is incorporated into the iron–vanadium-oxide material; the caesium is not simply deposited on the surface of the materials. At low caesium loading the incorporation process is relatively facile, however, as the saturation point is approached it becomes more difficult.

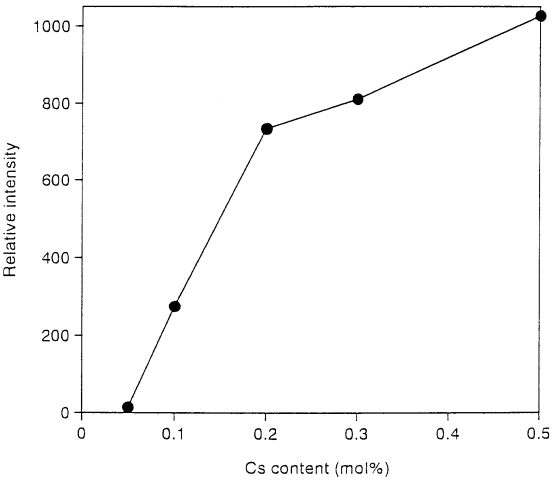

Fig. 3. Effect of amount of Cs dopant on the relative intensity of the $g' \approx 18$ peak for a constant V : Fe ratio of 1 : 0.74.

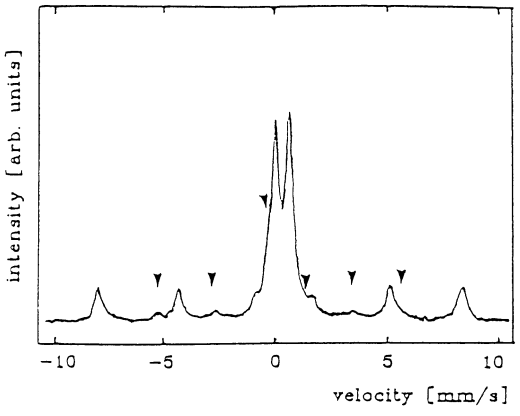

Fig. 2. Conversion electron Mössbauer spectrum of V : Fe : Cs = 1 : 0.74 : 0.06 sample showing the presence of iron sulphide, $Fe_{1-X}S$ (marked by arrows).

3.1.4. Effect of varying the alkali metal dopant

To determine the effect of different alkali metal dopants on the low-field ESR signal, iron–vanadium-oxide materials doped with rubidium or potassium were prepared. The rubidium-doped sample gave only a very small signal at $g' \approx 18$, compared with caesium, while no signal was observed for the potassium-doped sample (table 1).

The Mössbauer spectra obtained for the three different materials (figs. 4a–4c) have the three doublets associated with $FeVO_4$; however, on changing the alkali metal, the relative size of the doublets changed. The most obvious difference between the spectra can be seen when the outer two doublets are thought of as having a constant relative intensity; the central doublet can then be seen to decrease in intensity, relative to the other peaks, in the order K > Rb > Cs. In fact, with potassium as a dopant, only a small difference can be seen between the Mössbauer spectrum for the doped sample (fig. 4c) and the spectrum for amorphous $FeVO_4$ (fig. 1e).

The differences in the signal sizes seen in the Mössbauer spectra may be explained by the greater distortion of the local iron surrounding with respect to the standard $FeVO_4$. The doublet with the smallest quadrupole splitting, representing Fe^{3+} in a rather symmetric surrounding, decreases on moving from potassium ($r_i(K^+) = 1.51$ Å) to rubidium ($r_i(Rb^+) = 1.61$ Å) to caesium ($r_i(Cs^+) = 1.74$ Å). The more distorted iron sites, indicated by the Mössbauer spectra, agree with the appearance of the $g' \approx 18$ signal in the ESR spectra. The latter was found to arise from distorted iron sites described by a zero field splitting parameter, D, ranging

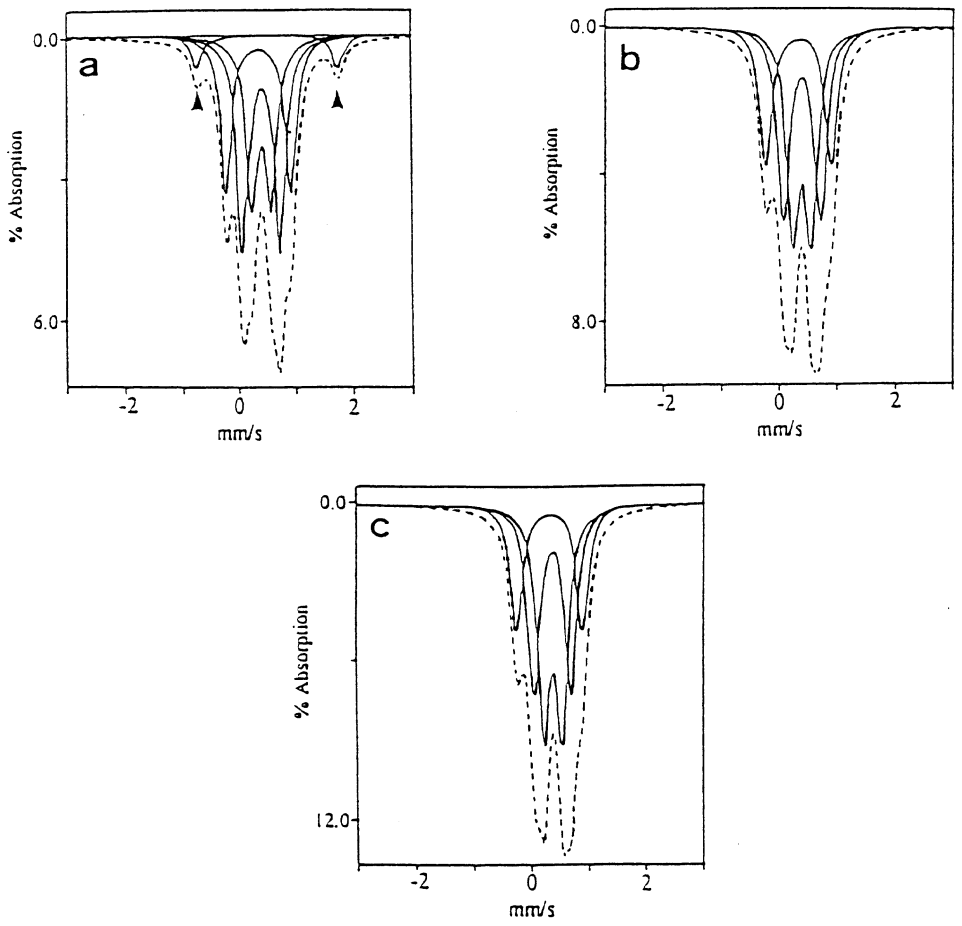

Fig. 4. Mössbauer spectra for the (a) Cs-, (b) Rb- and (c) K-doped samples (V : Fe= 1 : 0.74); α-Fe_2O_3 marked by arrows.

from 3600 to 4800 MHz [6,7]. The disappearance of this signal for potassium may be because the distortion around the Fe^{3+} is not great enough, leading to smaller D values. The appropriate signals are, thus, expected to occur in the range near $g' \approx 2$, and superimpose on that of $FeVO_4$ and $Fe_2V_4O_{13}$ so that only a broad signal at $g' \approx 2$ is seen, as in the case for the undoped sample. It was also shown by Brückner et al. that the low-field signal at $g' \approx 18$ is highly sensitive to small structural distortions, and that the materials contain Fe^{3+} species in close proximity to oxide vacancies, meaning that distortion of the iron ions could occur very easily. It is possible that, despite the total disappearance of the $g' \approx 18$ signal for the potassium-doped material, the addition of potassium does result in the formation of a similar phase, while also modifying the surface acidity. Indeed, according to the work by Baerns and co-workers [2,4], potassium also has a positive effect on the catalytic results (although not as great as for caesium) for the selective oxidation of polyaromatics.

3.2. Scanning electron microscopy

Figs. 5a–5c show scanning electron micrographs of typical areas of the caesium-doped V : Fe= 1 : 0.74 sample. Three different materials are seen: (i) long needle-like crystals (figs. 5a and 5b), identified as $FeVO_4$; (ii) large rectangular crystals (figs. 5a and 5c), $Fe_2V_4O_{13}$; and (iii) an amorphous material. EDX measurements indicated that the caesium was only associated with the amorphous material [19], and elemental mapping appears to further confirm this (see fig. 6d). The mapping also suggests that sulphur (fig. 6c) is present in the same areas as caesium, probably in the form of $Fe_{1-X}S$; this is expected since these elements are introduced together as Cs_2SO_4. The maps for iron and vanadium, shown in figs. 6a and 6b, respectively, indicate that these elements are distributed fairly uniformly; the black spot at the centre of the vanadium map corresponds to a dark spot in the iron map, and this can be explained by the presence of a small particle of α-Fe_2O_3.

3.3. Catalytic testing

In previous investigations, it was found that the oxidation of fluorene to 9-fluorenone could be carried out over Cs-doped V_2O_5–Fe_2O_3 catalysts, with selectivities as high as 99% [3]. In the present work, some of the materials discussed above have been tested for this reaction, in order to confirm our earlier interpretations and to check

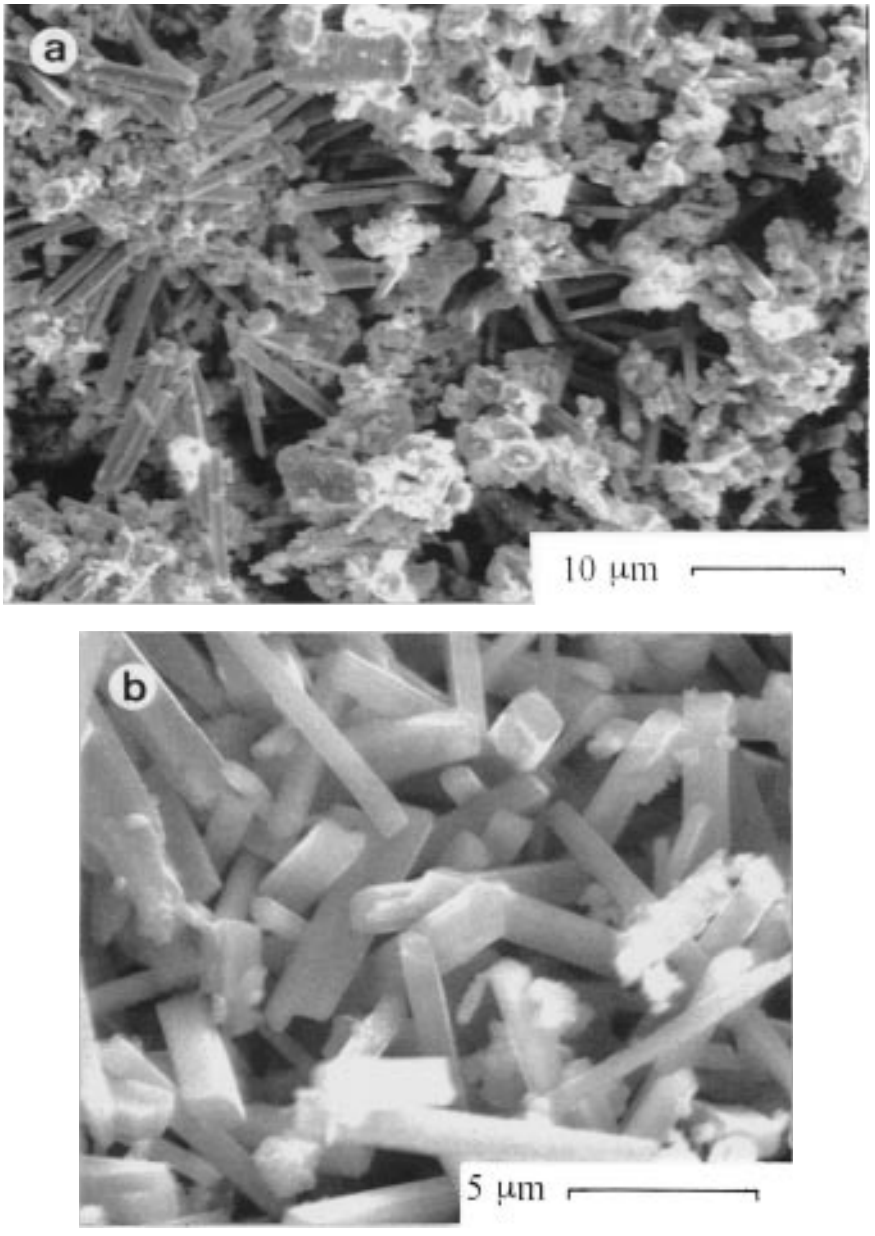

Fig. 5. Scanning electron micrographs of a Cs-doped Fe–V–O material (V : Fe : Cs= 1 : 0.74 : 0.06). (a) Overall background; (b) $FeVO_4$ crystals; and (c) $Fe_2V_4O_{13}$ crystal. (Continued on next page.)

the catalytic influence of $Fe_{1-X}S$, which has only recently been detected on the catalyst surface. The results obtained are presented in fig. 7, as a plot of 9-fluorenone selectivity as a function of total fluorene conversion. The lowest 9-fluorenone selectivities were exhibited by both the undoped sample and the $(NH_4)_2SO_4$-doped sample, with the results for these catalysts very similar; doping with both CsCl and Cs_2SO_4 resulted in an enhancement of the selectivity. These results confirm that the addition of sulphur to the materials is not effective in improving the catalyst performance, and therefore that the $Fe_{1-X}S$ is not an important catalyst component. However, the addition of caesium has a marked effect on the product selectivity. The highest selectivity was obtained using the V : Fe : Cs = 1 : 1 : 0.06 sample, with a substantial increase in the 9-fluorenone selectivity, compared with the CsCl-doped sample. The reasons for this marked improvement are unclear at present and further testing is needed. It is possible, however, that the dopant anion, although having no role in the catalytic processes occurring on the catalyst, does play a part in the synthesis of the catalyst, while the chloride may have a negative effect on the oxidation of polyaromatics, partially counteracting the positive effect of the caesium dopant.

Finally, it should be noted that at high conversion, for all the catalysts tested, the selectivity decreases due to the increased contribution of secondary reactions, leading to the destruction of the aromatic ring system and the formation of carbon oxides.

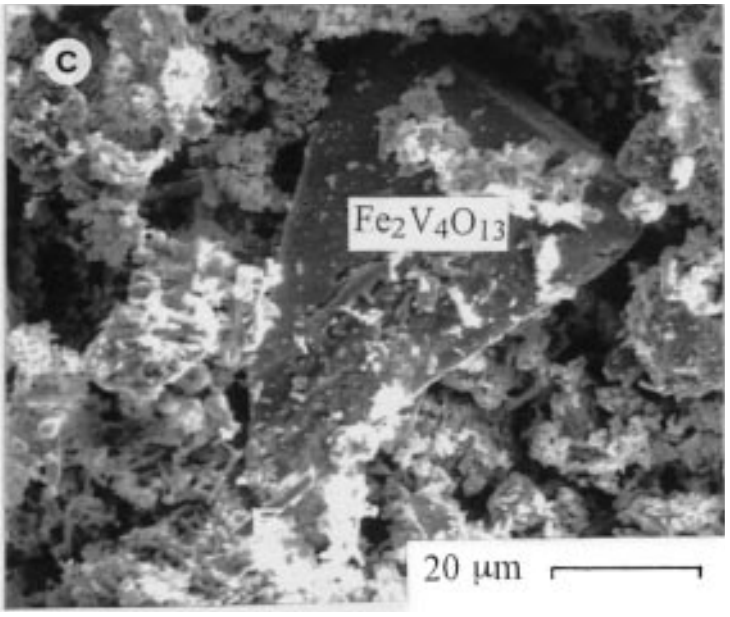

Fig. 5. (Continued.)

4. Discussion

The major difference between the ESR spectra of the undoped and caesium-doped iron–vanadium-oxide materials is the appearance of a low-field line ($g' \approx 18$) of high intensity; this arises exclusively when caesium is added to the materials, and is due to Fe^{3+} next to an oxygen vacancy occupied by an electron [6,7]. We propose that the caesium may be partially incorporated in some of the cationic lattice positions, leading to the formation of oxide vacancy species and a large distortion of the lattice, which can be seen as: (i) a low-field

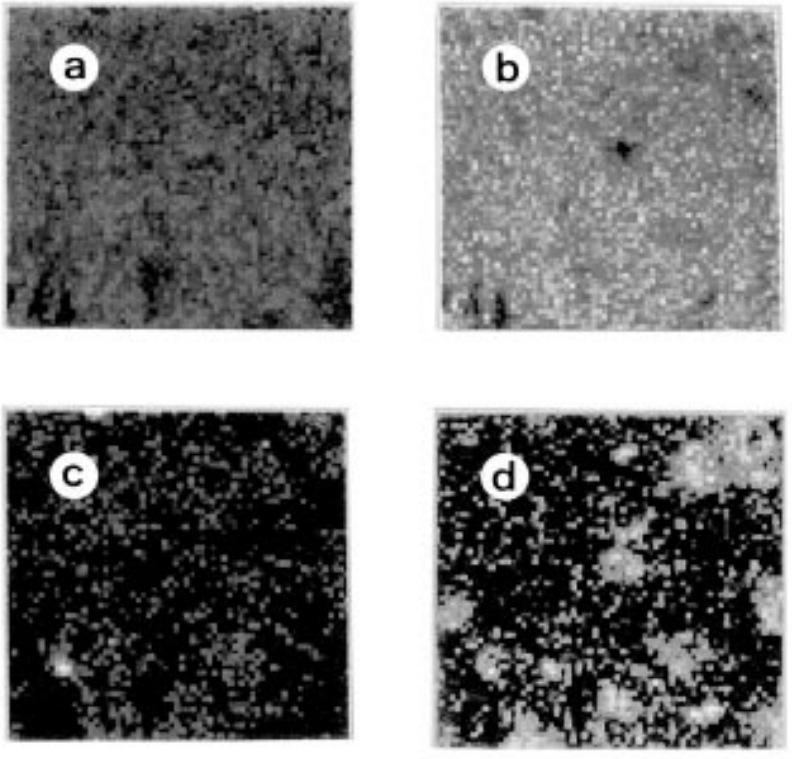

Fig. 6. Elemental mapping of the Fe–V–O material (V : Fe : Cs= 1 : 0.74 : 0.06). (a) Iron map; (b) vanadium; (c) sulphur; and (d) caesium.

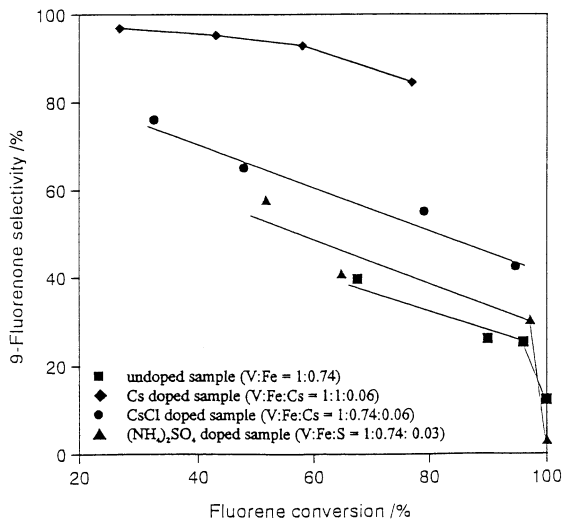

Fig. 7. 9-fluorenone selectivity vs. total fluorene conversion, $T = 633$ K.

ESR signal due to the Fe^{3+} sites in the neighbourhood of distorted oxide vacancies; and (ii) a shift in the relative intensities of the lines in the Mössbauer spectra. It is likely that the caesium can penetrate only a small distance into the $FeVO_4$ lattice due to its relatively larger ionic radii, however, due to differences in ionic charge between Fe^{3+} and Cs^+ incorporation would also result in the formation of oxide vacancies. According to reports by a number of researchers, these vacancies are electron donor centres which can readily reduce dioxygen from the gas-phase [20–22], probably via intermediate species like O_2^-, O_2^{2-} and O^-, to nucleophilic oxide ions, i.e. O^{2-}, which are available at the surface for mild insertion into the hydrocarbon molecule allowing the aromatic ring system to remain intact. Further evidence for caesium incorporation in the iron–vanadium-oxide lattice was presented in a previous publication, where it was shown, using X-ray photoelectron spectroscopy, that the caesium is enriched in the surface of the material while the amount of iron is lowered [3].

Finally, the surface acidity was also shown to decrease on addition of caesium [3,4,7], so this may be an important effect, as has been shown in previous publications [2,4,23,24]. The beneficial effect of alkali metal doping increased in all these studies with the molar mass of the alkali metal, and is generally discussed in terms of decreasing acidity of the catalyst. Therefore, in accordance with the literature, we would expect that potassium and rubidium will also favour the selectivity, although to a lesser extent than caesium due to the lower basicity. Moreover, the oxide vacancies, if formed in the presence of potassium or rubidium, are presumably not as stable as in the neighbourhood of the large polarisable caesium ion.

5. Conclusions

The addition of caesium to an iron–vanadium-oxide material leads to a marked increase in the selectivity for the oxidation of fluorene to 9-fluorenone. It is proposed that this is due to: (i) reduced surface acidity on addition of alkali metal; and (ii) the formation of a selective, non-stoichiometric, amorphous phase, which contains oxide vacancies able to activate O_2 to selective oxygen species suitable for nucleophilic addition to the hydrocarbon molecule, such as O^{2-}. This phase is identified by a distinctive high-intensity low-field signal in the ESR spectrum, probably arising from lattice distortion around iron species in close proximity to oxide vacancies, i.e. Fe^{3+}–$V_O(e^-)$. The $Fe_{1-X}S$, detected on the surface of the caesium-doped samples, does not play a catalytic role in the improved selectivities observed.

Acknowledgement

We thank the Deutsche Forschungsgemeinschaft for partially supporting this work, and APEY is grateful to the DAAD for a fellowship. Mr. G.-U. Wolf is acknowledged for experimental support, and Professor M. Meisel for helpful discussions.

References

[1] H. Pines, in: *The Chemistry of Catalytic Hydrocarbon Conversion* (Academic Press, New York, 1981) p. 227.
[2] M. Baerns, H. Borchert, R. Kalthoff, P. Kässner and F. Majunke, Stud. Surf. Sci. Catal. 72 (1992) 57.
[3] F. Majunke, S. Trautmann and M. Baerns, Stud. Surf. Sci. Catal. 82 (1994) 749.
[4] F. Majunke, PhD Thesis, Ruhr-Universität Bochum, Germany (1993).
[5] B. Odening, P. Kässner and M. Baerns, in: *Proc. DGMK Conference on Selective Oxidations in Petrochemistry*, Goslar, p. 347.
[6] A. Brückner, G.-U. Wolf, M. Meisel, R. Stösser and H. Mehner, J. Chem. Soc. Faraday Trans. 90 (1994) 3159.
[7] A. Brückner, G.-U. Wolf, M. Meisel, R. Stösser, H. Mehner, F. Majunke and M. Baerns, J. Catal. 154 (1995) 11.
[8] A.P.E. York, A. Brückner, G.-U. Wolf, M. Meisel and H. Mehner, in: *Proc. XXVIII Jahrestreffen deutscher Katalytiker*, Friedrichroda, p. 11.
[9] P. Murugaraj and T.R.N. Kutty, J. Mater. Sci. Lett. 5 (1986) 171.
[10] M. Touboul and D. Ingrain, J. Less-Common Metals 71 (1980) 55.
[11] M. Touboul and A. Popot, J. Therm. Anal. 31 (1986) 117.
[12] W. Meisel, Hyperfine Interact. 92 (1994) 1213.
[13] W. Meisel, H. Mehner and A. Brückner, Fresenius J. Anal. Chem. 352 (1995) 483.
[14] M. Baerns, R. Kalthoff, P. Kässner and A. Zein, in: *DECHEMA Monographie "Katalyse"*, Vol. 118, eds. H. Kral and D. Behrens (Verlag Chemie, Weinheim, 1989).
[15] A. Zein and M. Baerns, J. Chromatogr. Sci. 27 (1989) 249.
[16] B. Robertson and E. Kostiner, J. Solid State Chem. 4 (1972) 29.

[17] N.S. Ovanesyan, V.A. Trukhtanov, G.Yu. Odinec and G.V. Novikov, Zh. Eksp. Teor. Fiz. 60 (1971) 2220.
[18] H. Mehner, M. Lück, B. Essiger, C. Michalk and R. Stösser, Hyperfine Interact. 58 (1990) 2603.
[19] A.P.E. York, A. Brückner, G.-U. Wolf, P.-M. Wilde and M. Meisel, J. Chem. Soc. Chem. Commun. (1996) 239.
[20] A.G. Anshits, E.N. Voskresenskaya and L.I. Kurteeva, Catal. Lett. 6 (1990) 67.
[21] D.J. Ilett and M.S. Islam, J. Chem. Soc. Faraday Trans. 89 (1993) 3833.
[22] M.S. Islam, D.J. Ilett and S.C. Parker, J. Phys. Chem. 98 (1994) 9637.
[23] W.-D. Mross, Catal. Rev. Sci. Eng. 25 (1983) 591.
[24] D.V. Fikis, W.J. Murphy and R.A. Ross, Can. J. Chem. 56 (1978) 2530.